

Transforming spherical block polyelectrolyte micelles into free-suspending films *via* DNA complexation-induced structural anisotropy†

Cong Liu,^a Kaka Zhang,^a Daoyong Chen,^{*a} Ming Jiang^a and Shiyong Liu^{*b}

Received 13th April 2010, Accepted 30th June 2010

DOI: 10.1039/c0cc00902d

The deliberately prepared one ssDNA/one micelle complex has an unstable toroidal DNA-bound region and stable upper and lower hemispheres, and thus can self-assemble along the plane of the unstable toroidal region into free-suspending films.

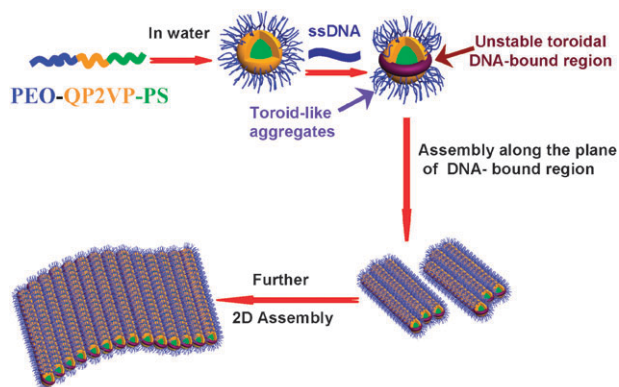
Self-assembly of molecules has emerged to be one of the most important strategies for constructing the nanostructures that can find important applications in various theoretical and applied fields.¹ Though a variety of zero- and one-dimensional aggregates have been prepared *via* molecular self-assembly, template-free fabrication of two-dimensional free-suspending films (FSFs) has been rarely reported. Recently, Lee *et al.*² reported a quite rare example in which FSFs were obtained from self-assembly of dumbbell-shaped rod amphiphiles, utilizing strong π - π interactions between the rod moieties. However, in most cases, molecular self-assembly cannot lead to FSFs since they, even though formed at a certain stage of the molecular self-assembly, lack sufficient rigidity and thus tend to further roll up into vesicles or tubes.³

On the other hand, inspired by hierarchical protein self-assembly in biological systems, the self-assembly of nanoparticles into superstructures has attracted much attention because nanoparticles are expected to be the “atoms” and “molecules” of tomorrow’s materials.⁴ Template-free self-assembly of nanoparticles with anisotropic interactions is of particular interest because it can lead to tailor-made complex superstructures.⁴ Nanoparticle self-assembly should also open new pathways for template-free formation of FSFs since the strong particle-particle interaction can make the resultant FSFs rigid enough to maintain their two-dimensional morphology in solutions.⁵ However, to form FSFs *via* template-free self-assembly of nanoparticles, specific anisotropic interactions between the nanoparticles is a prerequisite.^{5,6} It is noteworthy that for nanoparticles, especially for soft polymeric nanoparticles, the precise control over their anisotropic interactions has been a formidable task.

In the present study, we prepared highly flexible spherical nanoparticles bearing an unstable toroidal region at the periphery. As schematically described in Scheme 1, the

toroidal unstable regions of different spheres tend to fuse/aggregate with each other. This endows the spheres with such an anisotropic interaction that they self-assemble along the plane of the toroidal region and eventually form FSFs. This anisotropic interaction and the self-assembly behaviour are similar to those of the spheres with attractive equatorial ring-like patches described by Glotzer *et al.* based on computer simulation.^{5a} Furthermore, the spheres are highly flexible so that they were able to further fuse together along the plane of the FSF and thus to enhance the interaction between the building blocks. As a result, relatively large uniform FSFs were prepared, which can be stabilized in water for a long time.

The nanoparticles with the anisotropic interactions were deliberately prepared by complexation between single-stranded DNA (ssDNA) chains and spherical micelles consisting of a hydrophobic core, a positively charged inner shell, and a nonionic hydrophilic corona; the complexation occurred due to the ionic-ionic interaction between the positively charged inner shell and the negatively charged ssDNA chains in water. Under the conditions that the ssDNA chains are with an average contour length comparable to the perimeter of the spherical micelles, the ssDNA/micelle number ratio was kept to be 1 : 1.13 and the concentration of the block copolymer micelles is as low as 0.01 g L⁻¹, the complexation led to the complex in which one ssDNA chain wraps around one single micelle by interacting with the positively charged inner shell. The toroidal DNA-bound region becomes unstable due to charge neutralization, driving the two-dimensional self-assembly of the ssDNA/micelle complex along the plane of the toroidal DNA-bound region because the remaining top and bottom hemispheres were still protected by the nonionic hydrophilic corona (Scheme 1). As far as we know, this represents the first example of template-free two-dimensional



Scheme 1 Proposed mechanism and processes for the formation of a FSF.

^a The Key Laboratory of Molecular Engineering of Polymers and Department of Macromolecular Science, Fudan University, Shanghai, 200433, China. E-mail: chendy@fudan.edu.cn; Fax: (+86) 551-3607348; Tel: (+86) 021-65643989

^b CAS Key Laboratory of Soft Matter Chemistry, University of Science and Technology of China, Hefei, Anhui Province 230026, China. E-mail: sliu@ustc.edu.cn; Fax: (+86) 551-3607348

† Electronic supplementary information (ESI) available: Materials and instruments, DLS characterization of ssDNA/micelle complex, TEM images of FSFs obtained in different repeated experiments, TEM observation of the toroidal ssDNA/micelle complex after the staining with RuO₄. See DOI: 10.1039/c0cc00902d

assembly of soft polymeric nanoparticles into highly ordered two-dimensional superstructures.

Poly(ethylene oxide)-*b*-poly(2-vinylpyridine)-*b*-polystyrene triblock copolymer (PEO₇₁-P2VP₁₂-PS₂₉; $M_w/M_n = 1.10$; the subscripts represent degrees of polymerization for respective blocks) was fully quaternized with *n*-butyl iodide in DMF, leading to PEO₇₁-QP2VP₁₂-PS₂₉. Micelles of PEO₇₁-QP2VP₁₂-PS₂₉ were prepared by dropwise addition of water into the copolymer solution in DMF, followed by dialysis against water (S1, †ESI). The concentration of the final dispersion was 0.01 mg mL⁻¹. The critical micellization concentration of the triblock copolymer was determined to be 0.003 mg mL⁻¹ by a fluorescent technique using pyrene as a probe.⁷ Dynamic light scattering (DLS) analysis revealed an intensity-average hydrodynamic radius, $\langle R_H \rangle$, of 10.5 nm for the micelles. The apparent molar mass and average aggregation number, N_{agg} , of the micelles were 1.1×10^5 g mol⁻¹ and 15, respectively, as determined by static light scattering (SLS) measurements. Transmission electron microscopy (TEM) observations revealed spherical nanoparticles with an average diameter of 20 nm (Fig. 1a), which reasonably agrees with the size determined by DLS. The aggregation of the highly hydrophobic PS block chains in water led to the micellization. Obviously, the micelles are with a PS core, QP2VP as the inner shell and PEO as the corona.

ssDNA/micelle complex was prepared by mixing the micellar solution at the concentration of the copolymer of 0.01 mg mL⁻¹ with ssDNA (200 nucleotides and 68 nm in the contour length) to the number ratio of ssDNA chains to micelles of 1/1.13; the number of the micelles is slightly larger than that of the ssDNA chains. The solution mixture was transparent and stable upon standing for more than 4 weeks. DLS was applied to track the time evolution of the $\langle R_H \rangle$ of the ssDNA/micelle complex in water (S2, †ESI). Initially, we observed a slight increase of the $\langle R_H \rangle$ to 12 nm when measured immediately after mixing. At 10 min and 24 h after the mixing, the $\langle R_H \rangle$ further increased to ~100 nm and ~300 nm, respectively. This indicated the occurrence of secondary aggregation of the initially formed aggregates.

The morphology evolution of the aggregates has been further checked by TEM observations. Immediately after mixing, TEM observations revealed the presence of toroid-like aggregates (Fig. 1b),⁸ the average perimeter of which is comparable to that of the micelles and also contour length of the ssDNA chains; 2 h later, relatively small sheet-like aggregates can be observed (Fig. 1c). From the enlarged TEM image of the sheet-like aggregates (inset in Fig. 1c), a network superstructure, which seems to be constructed by two-dimensional fusion of circles along the plane of the circles, is visible. The size of each circle in the network is 8–10 nm. At ~24 h after mixing, large FSFs were formed in solution (Fig. 1d).[†] Magnified TEM images (the Inset in Fig. 1d) revealed a periodic network structure with a spacing period of ~8–10 nm in the FSFs. To further confirm the periodic network superstructure, we characterized the FSFs in water using small angle X-ray scattering (SAXS). As shown in Fig. 1e, the SAXS profile of the FSFs presents a reflection peak at a *d*-space of ~10 nm, which further confirms the periodic superstructure in the FSFs.

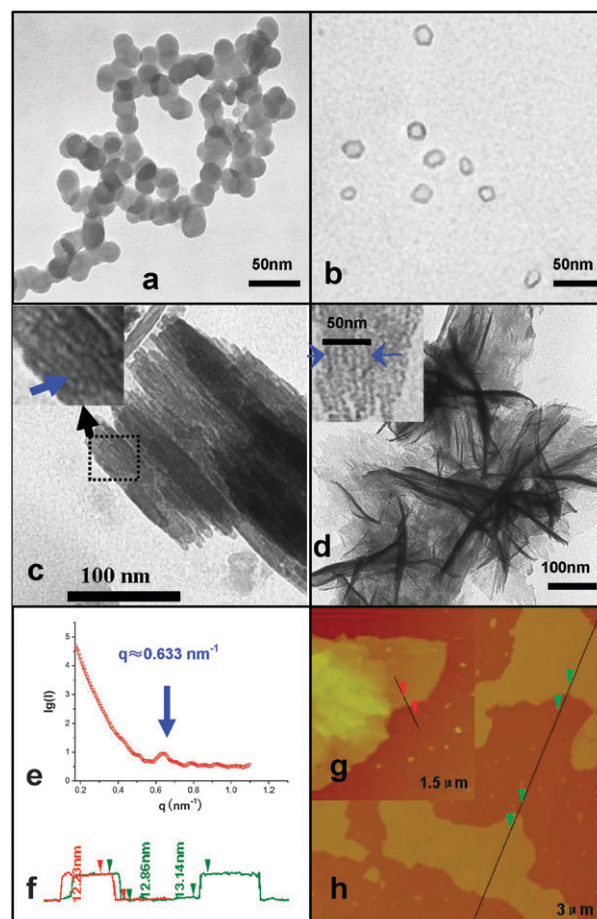


Fig. 1 TEM images of: (a) the micelles (stained with RuO₄); (b) the ssDNA/micelle complex (unstained); (c) aggregates formed in the intermediate stage of assembly of the toroidal complex (unstained); (d) FSF formed in the final stage of the assembly of the toroidal complex (unstained); (e) the SAXS profile of the FSFs; (f), (g) and (h) the thickness profiles and AFM images of the FSFs. The red and green lines in (f) are the height profiles obtained along the straight lines in (g) and (h), respectively. As indicated in the two insets in (c) and (d), a network superstructure with an average spacing period of 8–10 nm is visible.

In the TEM images without staining (Fig. 1b, c and d), the domains with a relatively high contrast are the ssDNA/QP2VP complex whose contrast was enhanced remarkably by I⁻ as the counterions of the pyridinium of the QP2VP component. Note that the lower contrast domains in the network in the TEM images are not empty but filled with the PEO and PS components that are invisible under TEM observation without staining. This is confirmed by the fact that after staining FSFs with RuO₄ no such difference in the contrast in the TEM images of FSFs can be observed (S3, †ESI), and also by AFM characterization results that the surface of the FSFs is rather smooth (Fig. 1g and h). The thickness of an FSF is 12–14 nm, which is comparable to the diameters of the toroid-like aggregates.

The facts that the ssDNA/micelle complex formed at the very beginning of the complexation is with a toroid-like morphology (Fig. 1b) and the average contour length of the ssDNA chains is close to the average perimeter of the

toroid-like aggregates and that of the micelles strongly suggest that the toroid-like aggregates consist of one micelle and one ssDNA chain with the latter wrapped around the former *via* the electrostatic interactions. We can calculate that the total positively charged pyridinium per micelle is ~ 180 . Thus, the formed one ssDNA chain/one micelle complex should be negatively charged considering that an ssDNA chain possesses 200 nucleotides. This should make further binding of an additional free ssDNA chain onto a one DNA/one micelle complex much more difficult than the binding onto an uncomplexed micelle. Besides, the micelle concentration is quite low (0.01 mg mL^{-1}), and the number ratio of ssDNA chains to micelles is 1/1.13. Therefore, it is quite reasonable to expect that a toroid-like aggregate typically consists of one ssDNA chain and one single micelle. In the literature, Wilson *et al.* studied the complexation between biotinylated dextran molecules and gold nanoparticles. It was demonstrated that through controlling the molecular weight of the biotinylated dextran molecules and the size of the gold nanoparticles, one polymer chain/one particle complex could be produced.⁹ In Fig. 1b, due to the presence of I^- as the counterions in the complexed region, the contrast of the periphery of the toroid-like aggregates was relatively high compared to the center region. As mentioned before, although with a much lower contrast, the central area of the toroid-like aggregates is not empty but filled with the PEO and the PS components that are invisible under TEM observation without staining (S4 in †ESI). This is indeed reasonable considering the fact that the core of the original micelles was formed by the highly hydrophobic PS block chains with a high glass transition temperature. Therefore, the PS core of the micelles should be able to keep its integrity during and after the complexation with the ssDNA as well as during the self-assembly of the ssDNA/micelle complex.

Comparing the periodic network superstructures of the small sheet-like aggregates formed at the intermediate stage and the FSFs as the final product with the toroid-like structure of the aggregates formed at the beginning of the ssDNA/micelle complexation as the starting material, the mechanism for forming FSFs is proposed as follows. In the structure of the toroid-like aggregates (Scheme 1), the toroidal DNA-bound region composed of ssDNA/QP2VP complex is unstable due to the charge neutralization, as demonstrated by the fact that complexes of a polyanion and a polycation are insoluble in water except that one of the polyelectrolytes is in large excess. As a result, the toroid-like aggregates tend to aggregate together to fuse the unstable toroidal complexed region together, whereas the remaining parts, namely the upper and lower hemispheres, are uncomplexed and still well-solvated and stable. Due to this structural anisotropy, the toroid-like aggregates can only self-assemble (fuse) along the plane of the toroidal DNA-bound region. This should finally lead to FSFs. It is noted that the spacing period of the network superstructures observed by TEM is 8–10 nm, which is close to the period revealed by the SAXS characterization (10 nm) but less than the size of the toroid-like aggregates observed by TEM (20 nm; Fig. 1b). This indicates that the toroid-like aggregates contracted remarkably after their fusion

for forming the sheet-like aggregates and FSFs. Actually, in our previous study, we also found that the size of the soft polymeric Janus nanoparticles decreased remarkably after they self-assembled into and further fused in superstructures.¹⁰

In conclusion, we prepared toroid-like ssDNA/micelle aggregates, in which one ssDNA chain wraps around one micelle with PEO as the corona, positively charged QP2VP as the inner shell and PS as the core, utilizing complexation between the ssDNA chain and the inner shell. The toroidal DNA-bound region is unstable whereas the upper and lower hemispheres of the toroidal aggregates are uncomplexed and stable. This endows the toroid-like aggregates with such a structural anisotropy that they can only self-assemble two-dimensionally along the plane of the toroidal DNA-bound region, finally leading to FSFs. The unique structural anisotropy of the toroid-like aggregates and the two-dimensional self-assembly make the present study significant in the fields of self-assembly, material and colloidal sciences.

The authors are grateful for financial support from NSFC (50825303, 50773011 and 30890140) and the Ministry of Science and Technology of China (2009CB930400).

Notes and references

† It should be mentioned here that the FSFs can be repeatedly prepared from self-assembly of the ssDNA/micelle complex in the aqueous solution. As described (see S1, †ESI), the specimens for TEM observations were dried under vacuum at -60°C for 72 h. Besides, in the TEM images, some FSFs are overlapped and corrugations can be seen in FSFs (S3, ESI). Therefore, the FSFs were formed in the aqueous solution.

- (a) D. E. Discher and A. Eisenberg, *Science*, 2002, **297**, 967; (b) D. J. Pochan, Z. Y. Chen, H. G. Cui, K. Hales, K. Qi and K. L. Wooley, *Science*, 2004, **306**, 94; (c) D. N. Reinhoudt and M. Crego-Calama, *Science*, 2002, **295**, 2403; (d) T. Gadit, N. S. Jeong, G. Cambridge, M. A. Winnik and I. Manners, *Nat. Mater.*, 2009, **8**, 144.
- J.-K. Kim, E. Lee, Y.-H. Jeong, J.-K. Lee, W. C. Zin and M. Lee, *J. Am. Chem. Soc.*, 2007, **129**, 6082.
- C. P. Collier, J. J. Shiang, S. E. Henrichs and J. R. Heath, *Science*, 1997, **277**, 1978.
- (a) A. Walther and A. H. E. Müller, *Soft Matter*, 2008, **4**, 663; (b) R. Erhardt, M. Zhang, A. Böker, H. Zettl, C. Abetz, P. Frederik, G. Krausch, V. Abetz and A. H. E. Müller, *J. Am. Chem. Soc.*, 2003, **125**, 3260–3267; (c) A. Walther, M. Hoffmann and A. H. E. Müller, *Angew. Chem., Int. Ed.*, 2008, **47**, 711; (d) H. W. Duan, D. Y. Wang, D. G. Kurth and H. Mohwald, *Angew. Chem., Int. Ed.*, 2004, **43**, 5639–5642; (e) S. C. Glotzer, *Science*, 2004, **306**, 419.
- (a) Z. L. Zhang and S. C. Glotzer, *Nano Lett.*, 2004, **4**, 1407; (b) S. C. Glotzer and M. J. Solomon, *Nat. Mater.*, 2007, **6**, 557; (c) S. Srivastava and N. A. Kotov, *Soft Matter*, 2009, **5**, 1146; (d) Z. Y. Tang, Z. L. Zhang, Y. Wang, S. C. Glotzer and N. A. Kotov, *Science*, 2006, **314**, 274.
- T. M. Hermans, M. A. C. Broeren, N. Gomopoulos, P. van der Schoot, M. H. P. van Genderen, N. A. J. M. Sommerdijk, G. Fytas and E. W. Meijer, *Nat. Nanotechnol.*, 2009, **4**, 721.
- E. A. Lysenko, T. K. Bronich, E. V. Slonkina, A. Eisenberg, V. A. Kabanov and A. V. Kabanov, *Macromolecules*, 2002, **35**, 6351–6361.
- H. G. Cui, Z. Y. Chen, K. L. Wooley and D. J. Pochan, *Soft Matter*, 2009, **5**, 1269–1278.
- R. Wilson, Y. Chen and J. Aveyard, *Chem. Commun.*, 2004, 1156.
- (a) L. Cheng, G. Z. Zhang, L. Zhu, D. Y. Chen and M. Jiang, *Angew. Chem., Int. Ed.*, 2008, **47**, 10171; (b) L. Nie, S. Y. Liu, W. M. Shen, D. Y. Chen and M. Jiang, *Angew. Chem., Int. Ed.*, 2007, **46**, 6321.